# Conditional saddle-point configurations

K. Thomas R. Davies
*Physics Division, Oak Ridge National Laboratory, Oak Ridge, Tennessee 37831*

Arnold J. Sierk
*Theoretical Division, Los Alamos National Laboratory, Los Alamos, New Mexico 87545*
*and Physics Division, Oak Ridge National Laboratory, Oak Ridge, Tennessee 37831*
(Received 9 November 1984)

A general method is presented for determining an equilibrium point on a potential energy surface subject to an arbitrary number of constraints. The method is then specialized to the calculation of a conditional saddle point in the liquid-drop model for which the constraint is the mass-asymmetry degree of freedom. This approach is useful for cases in which the mass asymmetry is not one of the chosen coordinates but instead is a function of these coordinates. Conditional saddle points are calculated for the liquid-drop and Yukawa-plus-exponential nuclear energy models, with the nuclear shape parametrized using both a three-quadratic-surface model and a Legendre polynomial expansion of the nuclear surface function. We show how the conditional saddle-point shapes and energies change as the fissility $x$ and the mass asymmetry value $\alpha$ are varied. As $\alpha$ increases for fixed $x$, the saddle-point configurations effectively behave like lighter (less fissile) nuclei. For fissilities less than the Businaro-Gallone value ($x_{BG}$), the conditional saddle-point energy always decreases with increasing $\alpha$. For $x > x_{BG}$, with increasing $\alpha$ the conditional saddle-point energy increases until it reaches the limit of the Businaro-Gallone peak, after which the energy decreases.

## I. INTRODUCTION

One interesting development in heavy-ion physics has been the study of dynamical thresholds for the onset of fusion.[1–54] Such thresholds, associated with the phenomenon called the extra push,[20–23] appear whenever the repulsive energy of the system is sufficiently high, causing the fission saddle point to be correspondingly compact. It is well established that, for a head-on collision of a sufficiently light system, fusion will always occur if the center-of-mass (c.m.) bombarding energy is greater than or equal to the height of the interaction barrier. However, for a fixed c.m. energy above the barrier, fusion becomes less probable as one increases the repulsion of the system (by increasing either the charge of the projectile or target or by increasing the orbital angular momentum). Therefore, above a certain critical fissility or above a critical angular momentum value, fusion does not automatically occur. Then, e.g., for a head-on collision of a system whose fissility exceeds the critical fissility, fusion will occur only if the difference between c.m. bombarding energy and the interaction barrier height is greater than a certain threshold value. (This difference is sometimes called the extra-push energy.[20–23]) Such a dynamical threshold depends critically upon the total charge, the orbital angular momentum, and the mass asymmetry of the system;[13,20–23,25] additional detailed behavior of the thresholds is being studied theoretically using both macroscopic[49–53] and microscopic[52,54] approaches. Recently, it has been determined that the threshold behavior can be very sensitive to some assumptions of the models used.[25,49–53] For example, macroscopic studies[49–52] show that the fusion behavior depends critically upon the type of dissipation assumed, whereas in the microscopic time-dependent Hartree-Fock approximation[29,52,54] the fusion thresholds can differ dramatically for different two-body effective interactions.

In most of the macroscopic theoretical studies,[8–26,49–52] a particular approach has been used to determine the dynamical fusion thresholds. For simplicity in explaining this method, we shall first consider the case of a mass symmetric reaction. The following criterion has been adopted to determine whether fusion occurs. The dynamical trajectory for the reaction is plotted in a multidimensional configuration space, and it is asumed that a true compound nucleus is formed if this trajectory passes inside of the saddle point for the combined system. This assumption is based on the argument that, due to dissipation effects and coupling to higher collective modes, there is a loss of kinetic energy in the reseparation degree of freedom, and the system becomes trapped in the potential energy hollow between the ground-state and saddle-point configurations. However, if the dynamical path passes outside of the saddle point, then it is assumed that the system reseparates, giving rise to quasielastic or deep-inelastic scattering.

Now consider the case of a mass asymmetric reaction. Then, as Swiatecki[20–23] has emphasized, there are two different saddle points which can differentiate between two types of long-lived coalesced configurations. First, there is the true (or Bohr-Wheeler) saddle point for the combined system. In addition, there is the conditional saddle point which is obtained by finding a point of equilibrium on the potential energy surface subject to the constraint that the mass asymmetry be fixed at the initial value for the reaction. As before, if the dynamical trajec-

 

tory for the system, plotted on a multidimensional configuration space, passes inside the Bohr-Wheeler saddle, it is assumed that a compound nucleus is formed. However, according to Swiatecki,[20–23] dynamical trajectories which lie *between* the Bohr-Wheeler and the conditional saddle points correspond to a special longer-lived process known as fast fission or quasifission. Also a distinction can be made between energies associated with the extra push and the extra-extra push.[20–23] The extra-push energy is the minimum value required to reach the conditional saddle point, while the extra-extra push energy is the minimum value required to reach the Bohr-Wheeler saddle. The fast fission process has a reaction time estimated to be of the order of $10^{-20}$ sec, and it is thought to be intermediate between true compound nucleus formation and a deep-inelastic reaction. This definition of fast fission is useful in the sense that it enables one to distinguish theoretically fast fission from other reaction processes. In order for the conditional saddle point to determine the onset of fast fission, it is necessary that the characteristic time for mass transfer between the interacting nuclei be much longer than the times characteristic of the other collective modes. We should note that in other theoretical approaches[45–47] fast fission may arise in a different way. Presumably the best way[53] to determine theoretically whether fast fission has occurred is to use a very general macroscopic shape parametrization[55] in order to follow the reaction indefinitely; then, if the system eventually reseparates, the mass transfer, the energy dissipated, and the total reaction time can be accurately estimated. However, there is a clear need to study the role of the conditional saddle point in fusion dynamics.

In the first studies[20–25] involving conditional saddle points, the mass asymmetry variable was a member of the set of coordinates chosen, which enabled the extremum to be easily calculated. In general, such a simplification may not be convenient or possible, and the mass asymmetry will be a function of the chosen coordinates. One purpose of this paper is to present a numerical method for calculating the conditional saddle point for a general function describing the nuclear shape. We shall also present results showing the behavior of the conditional saddle-point shapes and energies as the fissility and the initial mass asymmetry values are varied.

The structure of this paper is as follows. In Sec. II we develop a general method for finding an extremum on the potential energy surface subject to an arbitrary number of constraints, and this method is specialized to the case involving the single constraint of mass asymmetry. Then, in Sec. III we present the calculated results showing the systematic behavior of conditional saddle-point shapes and energies. Finally, in Sec. IV we briefly summarize our results.

## II. METHOD FOR CALCULATING CONSTRAINED EQUILIBRIUM POINTS

### A. General method

In the usual method of calculating equilibrium points in classical mechanics[56] (e.g., saddle point or ground-state configurations), one finds that the potential energy satisfies the equation

$$\frac{\partial V}{\partial q_i}(q_1,q_2,\ldots,q_N)=0\ ;\quad i=1,2,\ldots,N\ , \tag{2.1}$$

where $q\equiv q_1,q_2,\ldots,q_N$ are a set of $N$ generalized coordinates specifying the shape of the system. A method for solving Eq. (2.1) is the vector version of Newton's method which gives[55]

$$q_i^{(I+1)}=q_i^{(I)}-\sum_{j=1}^{N}(K^{-1})_{ij}^{(I)}\left[\frac{\partial V(q)}{\partial q_j}\right]^{(I)}\ ;\quad i=1,2,\ldots,N\ , \tag{2.2}$$

where

$$K_{ij}=\frac{\partial^2 V(q)}{\partial q_i\partial q_j} \tag{2.3}$$

is the symmetric curvature matrix. The superscripts $I$ and $I+1$ in Eq. (2.2) refer to the Newton's method iterations $I$ and $I+1$.

We now generalize Eqs. (2.1)—(2.3) to the case in which the equilibrium is subject to certain constraints. In particular, we demand that

$$\delta V(q)=\sum_{i=1}^{N}\frac{\partial V(q)}{\partial q_i}\delta q_i=0\ , \tag{2.4}$$

with the constraints

$$Q_i(q)=Q_i^{(0)}\ ;\quad i=1,2,\ldots,n\ , \tag{2.5}$$

where the $Q_i$ are $n<N$ *specified* functions of the coordinates and the $Q_i^{(0)}$ are constants. The $\delta q_i$ in Eq. (2.4) are variational displacements. From Eq. (2.5) we also have

$$\delta Q_i=\sum_{j=1}^{N}\frac{\partial Q_i}{\partial q_j}\delta q_j=0\ ;\quad i=1,2,\ldots,n\ . \tag{2.6}$$

The required variational expression is then given by

$$\frac{\partial V}{\partial q_i}+\sum_{j=1}^{n}\lambda_j\frac{\partial Q_j}{\partial q_i}=0\ ;\quad i=1,2,\ldots,N\ , \tag{2.7}$$

with the $n$ Lagrange multipliers $\lambda_j$.

We first note that in Eqs. (2.5) and (2.7) there are $N+n$ quantities to be determined, namely

$$q_1,q_2,\ldots,q_N$$

and

$$\lambda_1,\lambda_2,\ldots,\lambda_n\ .$$

We solve Eqs. (2.5) and (2.7) using a special iterative method. We initially choose $N$ $q$'s and then solve for the $n$ $\lambda$'s, after which we can use Newton's method to obtain a new set of $N$ $q$'s. This iteration procedure is continued until we obtain convergence. Whether and how rapidly the iterations converge clearly depends on the initial choice of the $q$'s. Suppose that

$$q_1^{(I)}=q_2^{(I)}\ ,q^{(I)},\ldots,q_N^{(I)}$$

are the coordinates to be used for iteration $I$. Then we can obtain the $n$ $\lambda$'s by solving the linear inhomogeneous equations

$$\sum_{j=1}^{n}\lambda_j^{(I)}\left[\frac{\partial Q_j}{\partial q_i}\right]^{(I)}=-\left[\frac{\partial V}{\partial q_i}\right]^{(I)};\quad i=1,2,\ldots,n\ , \tag{2.8}$$

where again the superscript $I$ refers to iteration $I$. We next define the column vector $\eta$ whose components are given by

$$\eta_i=Q_i(q)-Q_i^{(0)};\quad i=1,2,\ldots,n \tag{2.9a}$$

$$\eta_i=\frac{\partial V}{\partial q_i}+\sum_{j=1}^{n}\lambda_j\frac{\partial Q_j}{\partial q_i};\quad i=n+1,n+2,\ldots,N\ , \tag{2.9b}$$

and we require that

$$\eta_i^{(I)}=0\ ,\quad i=1,2,\ldots,N\ . \tag{2.10}$$

Using the vector Newton's method, we obtain

$$q_i^{(I+1)}=q_i^{(I)}-\sum_{j=1}^{N}(\tau^{-1})_{ij}^{(I)}\eta_j^{(I)}\ , \tag{2.11}$$

where the *nonsymmetric* matrix $\tau$ is defined as

$$\tau_{ij}=\frac{\partial\eta_i}{\partial q_j}\ . \tag{2.12}$$

Note too that in Eq. (2.8) we have used the *first* $n$ equations of Eq. (2.7) to obtain the $n$ Lagrange multipliers, and then the remaining $N-n$ equations of Eq. (2.7) are satisfied using Eqs. (2.9)—(2.12). It should be emphasized that this choice is completely arbitrary and is only chosen for ease of presentation. Obviously, *any* $n$ equations of Eq. (2.7) could be used for Eq. (2.8), with the remaining $N-n$ equations used in Eq. (2.9b). In fact, for physical reasons it may be quite desirable in Eq. (2.7) to choose a particular subset for determining the Lagrange multipliers.

### B. Conditional saddle points

A conditional saddle point[20–23] is defined as an extremum in the potential energy surface subject to the constraint

$$Q_i(q)=Q_i^{(0)}\ , \tag{2.13}$$

where the vector components $Q_i^{(0)}$ are constants. In the general case, one might choose the $Q_i$'s to be multipole moments, for example. For the rest of this paper, we will specialize to the case of $Q(q)=\alpha(q)$, where $\alpha(q)$ is a function specifying the mass asymmetry of the system. For example, a convenient definition of $\alpha$ is given by

$$\alpha(q)=\frac{M_R(q)-M_L(q)}{M_R(q)+M_L(q)}\ , \tag{2.14}$$

where $M_R$ and $M_L$ are the masses of the nuclear fluid to the right and left, respectively, of a plane passing through the neck region of the body. Obviously this prescription only makes sense for nuclear shapes for which a well-defined neck exists. If $\alpha$ is chosen to be one of the generalized coordinates, as in Refs. 20—25, the calculation of conditional saddle points is greatly simplified. Such a choice is not always possible or convenient, and here we present the general case in which $\alpha$ is a function of the $N$ coordinates. The solution of this problem is clearly a special case of the method outlined in Sec. II A.

The set of equations to be solved is given by

$$\frac{\partial V}{\partial q_i}+\lambda\frac{\partial\alpha}{\partial q_i}=0\ ;\quad i=1,2,\ldots,N\ . \tag{2.15}$$

We pick one of the coordinate indices for convenience, say $i=1$, and solve for the single Lagrange multiplier

$$\lambda=-(\partial V/\partial q_1)/(\partial\alpha/\partial q_1)\ . \tag{2.16}$$

We next define the $\eta$ vector

$$\eta_1=\alpha(q)-\alpha^{(0)}\ , \tag{2.17a}$$

$$\eta_i=\frac{\partial V}{\partial q_i}+\lambda\frac{\partial\alpha}{\partial q_i};\quad i=2,3,\ldots,N\ , \tag{2.17b}$$

and then determine the equilibrium coordinates by iterating using Eqs. (2.10)—(2.12).

For axially symmetric shapes, we now show how to evaluate the quantity $\partial\alpha/\partial q_i$ appearing in Eqs. (2.16) and (2.17b). Equation (2.14) can be expressed in cylindrical coordinate $(\rho,z)$ as

$$\alpha(q)=(V)^{-1}\pi\left[\int_{z_{\rm neck}}^{z_{\rm max}}P^2(z;q)dz-\int_{z_{\rm min}}^{z_{\rm neck}}P^2(z;q)dz\right]\ , \tag{2.18}$$

where $V$ is the total (constant) volume of the system; $z$ is the coordinate along the symmetry axis; $P(z;q)$ is the value of the cylindrical coordinate $\rho$ on the surface at point $z$; and $z_{\rm min}$, $z_{\rm max}$, and $z_{\rm neck}$, are, respectively, the $z$ values for the minimum, maximum, and neck positions of the sharp surfaced shape. Conservation of volume implies the relation

$$\frac{\partial}{\partial q_i}\left[\int_{z_{\rm neck}}^{z_{\rm max}}P^2(z;q)dz\right]=-\frac{\partial}{\partial q_i}\left[\int_{z_{\rm min}}^{z_{\rm neck}}P^2(z;q)dz\right]\ , \tag{2.19}$$

and we find that

$$\frac{\partial\alpha(q)}{\partial q_i}=2\pi V^{-1}P^2(z_{\rm neck};q)A_i(z_{\rm neck};q)\ , \tag{2.20}$$

where

$$A_i(z;q)=[P(z;q)]^{-2}\frac{\partial}{\partial q_i}\int_z^{z_{\rm max}}P^2(z',q)dz' \tag{2.21}$$

is the shape-dependent Werner-Wheeler coefficient[57] occurring in various *dynamical* studies of fission and heavy-ion reactions. In such studies the inertia and viscosity tensors are calculated using $A_i$ and its derivatives with respect to $z$. However, we emphasize that determining the location of the conditional saddle point is purely a *static* problem, depending only on the shape of the potential energy surface and the functional form of $\alpha$.

## III. CALCULATED RESULTS

We now present the results of calculations of conditional saddle points using the method described in Sec. II. The shape-dependent potential energy $V(q)$ is the sum of two parts,

$$V(q)=V_{\text{Coul}}(q)+V_{\text{nucl}}(q)\ , \tag{3.1}$$

where $V_{\text{Coul}}$ is the Coulomb electrostatic energy[58] and $V_{\text{nucl}}$ is either the surface energy of the liquid-drop model,[59] or the Yukawa-plus-exponential double-folded nuclear energy.[60,61] Most of the results in this paper are presented for the liquid-drop model because numerical calculations are much simpler with this model. However, we also present results using a model with the Yukawa-plus-exponential nuclear energy and the Coulomb energy of diffuse-surfaced nuclei, showing that the results are qualitatively similar in the two models.

We use two shape parametrizations for these calculations: the three-quadratic-surface parametrization[57,62] which has $N=5$, and the asymmetric Legendre-polynomial parametrization[55,53] for which we use $N=24$ for the liquid-drop model and $N=6-10$ for the diffuse-surfaced model. The potential energy $V(q)$ is calculated by means of Gaussian quadrature formulas, where the liquid-drop model surface energy is a one-dimensional integral,[55] the Coulomb energy is a two-dimensional integral,[55,58] and the Yukawa-plus-exponential energy and the diffuseness corrections to the Coulomb energy are three-dimensional integrals.[61] The integrals along the nuclear symmetry axis use 64- or 128-point quadrature formulas, while the angular integrals in the diffuse-surface model use a 32-point formula. In the calculations involving the Legendre-polynomial parametrization, the energies and the first and second derivatives are all calculated by performing the appropriate Gaussian quadratures. When using the three-quadratic-surface parametrization, we calculate the second derivative matrix $K_{ij}$ [Eqs. (2.3) and (2.12)] by taking numerical derivatives of the $\partial V/\partial q_i$ vector, which is found by quadrature. We do not use Eq. (2.20) to evaluate $\partial\alpha/\partial q_i$ occurring in Eqs. (2.15)—(2.17); instead this quantity is found analytically in the case of the three-quadratic-surface parametrization, and numerically in the case of the Legendre-polynomial parametrization.

In order to present results of these multidimensional calculations, we project our results onto the two-dimensional space of mass moments $r$ and $\sigma$, where[8,9,57]

$$r\equiv\langle\,|z|\,\rangle_L+\langle\,|z|\,\rangle_R \tag{3.2}$$

and

$$\sigma\equiv[\langle z^2\rangle_L-\langle\,|z|\,\rangle_L^2]^{1/2}+[\langle z^2\rangle_R-\langle\,|z|\,\rangle_R^2]^{1/2}\ . \tag{3.3}$$

In Eqs. (3.2) and (3.3), $z$ is the coordinate along the nuclear symmetry axis, and the angular brackets denote averages over the partial masses to the left ($L$) and right ($R$) of the plane perpendicular to the $z$ axis passing through the region between the masses where the neck radius is a minimum. The moment $r$ gives the separation of the mass centers of the two partial masses, while $\sigma$ is a measure of the fragment elongation or necking of the shape. We wish to emphasize that these moments $r$ and $\sigma$ and the mass asymmetry $\alpha$ are not defined for a shape with no neck. Although some parametrizations[20,25] have a mass asymmetry coordinate defined even when there is no neck present, we feel that for the present purposes it is misleading to refer to a mass asymmetry coordinate for shapes which are so compact they do not have a well defined neck.

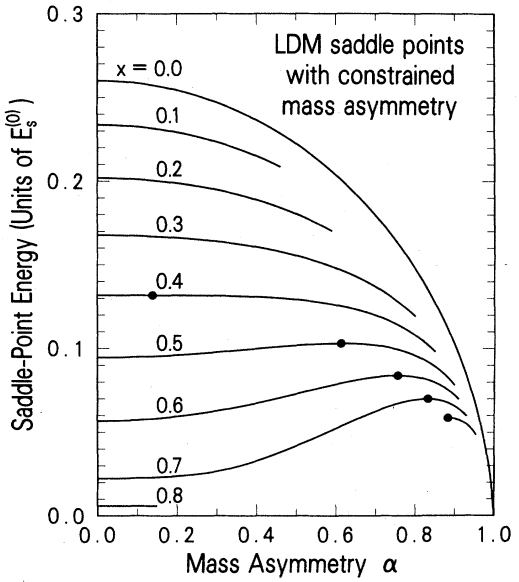


FIG. 1. Saddle-point energies as a function of constrained mass asymmetry for various values of the liquid-drop-model fissility parameter $x$. The solid points correspond to the Basinaro-Gallone family of asymmetric saddle-point shapes with two unstable degrees of freedom. The solid lines terminate to the right at shapes with very small neck radii, beyond which we cannot calculate. The curve for $x=0.8$ is not drawn where no constrained saddle point exists.

In Fig. 1 we show the calculated potential energies of saddle points with constrained mass asymmetry in the liquid-drop model. The energies are given as functions of the mass asymmetry $\alpha$ and parametrically as a function of the fissility $x$, where[57]

$$x=\frac{E_c^{(0)}}{2E_s^{(0)}}\ , \tag{3.4}$$

and $E_c^{(0)}$ and $E_s^{(0)}$ are the Coulomb and surface energies for a spherical nucleus. The values of the energies for $\alpha=0$ correspond to the Bohr-Wheeler family of symmetric binary saddle points. For fissility values $x<x_{\text{BG}}=0.396$, the symmetric Bohr-Wheeler saddle points have, in addition to the fission instability, a second mass-asymmetric instability. For $x>x_{\text{BG}}$, there exists a separate family of mass asymmetric saddle points of higher energy than the symmetric family. These mass asymmetric saddle points have two degrees of instability and are referred to as the Businaro-Gallone (BG) family.[63] The energies of these configurations are indicated on the figure as solid points. These *unconstrained* Businaro-Gallone saddle points lie exactly on the maxima of the potential energy curves of the *constrained* saddle points. We note that for $x<x_{\text{BG}}$, the potential energy always decreases as $\alpha$ increases from 0 to 1. For $x$ near $x_{\text{BG}}$ (e.g., $x=0.4$) the potential energy is almost exactly flat until $\alpha$ becomes quite large. For $x>x_{\text{BG}}$, the energy rises initial-

ly with increasing $\alpha$ until the Businaro-Gallone configuration is reached, then decreases as $\alpha$ approaches 1. For all values of fissility shown, the limiting configuration at $\alpha=1$ is a sphere with an infinitesimally small sphere tangent to it. The energy of this configuration is exactly equal to that of the ground state, or 0.0 on the figure.

In Fig. 2 we show the intersection of the axially symmetric nuclear shapes with a plane containing the axis of symmetry for $x=0.1$, 0.3, 0.5, and 0.7. The shapes are displayed for $\alpha$ values from 0.0 to the maximum value for which we could calculate a constrained saddle point. These shapes are shown in $\alpha$ intervals of 0.2 except for the last (dotted) one. We cannot calculate systems with larger values of $\alpha$ due to an inability to make the required numerical calculations for shapes with very small necks, even though such shapes exist. It is clear that the constrained saddle point shapes are approaching the limit of two tangent spheres for $\alpha$ approaching 1.0. One other noteworthy result is the elongation of the $x=0.7$ shapes as $\alpha$ increases from 0 to 0.4 with a subsequent shortening for $\alpha$ values greater than 0.4.

This effect is also apparent in Fig. 3, where in the upper portion we show, in the space of moments $r$ and $\sigma$, the locations of the symmetric saddle points for $0.0\leq x\leq 0.7$. As one decreases the fissility, the saddle point shapes become first more elongated, then for $x\lesssim 0.6$, more compact. In the lower portion, we show for $x=0.7$ the locations of the constrained saddle points for values of $\alpha$ from 0.0 to 0.93. As $\alpha$ is increased, the locus of saddle points with constrained mass asymmetry for $x=0.7$ closely follows the Bohr-Wheeler curve shown in the upper part of the figure. In general, for $x>0.60$ as $\alpha$ increases, the conditional saddle moves first to the right until it reaches the neighborhood of the bend in the liquid-drop-model curve shown in the upper part of Fig. 3, after which it moves to the left becoming more compact. For moderately heavy systems, this initial displacement of the conditional saddle point toward more elongated shapes is thought to be the mechanism allowing fast fission to occur more readily when the mass asymmetry is increased.[20,25] For $x\lesssim 0.60$, as $\alpha$ increases the conditional saddle point always moves roughly along the curve to the left toward more compact shapes. All of these results further demonstrate the observation[20,25] that the effective fissility of a nuclear system decreases as the mass asymmetry increases.

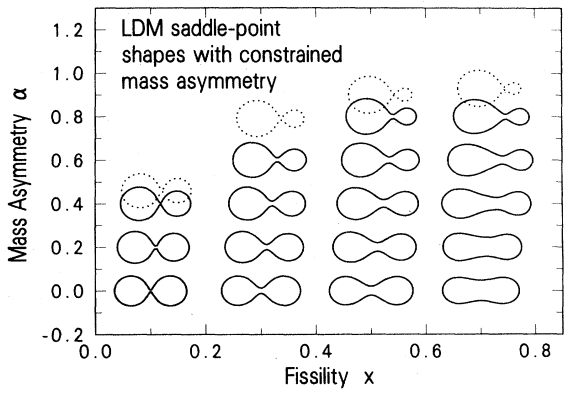


FIG. 2. Liquid-drop-model saddle-point configurations for the fissilities $x=0,1$, 0.3, 0.5, and 0.7 and for various values of constrained mass asymmetry $\alpha$. The centers of mass of the shapes are located at the appropriate values of $x$ and $\alpha$. For each value of $x$, the dotted shape, which has a very small neck radius, corresponds to the largest value of $\alpha$ that we are able to calculate.

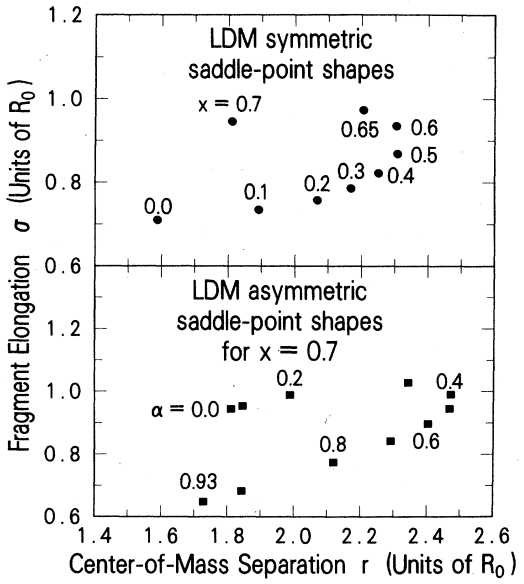


FIG. 3. Locations in $\sigma$-$r$ space of the saddle points of liquid-drop nuclei. The upper portion of the figure shows the positions of the Bohr-Wheeler family of symmetric saddle points for selected values of the fissility parameter $x$. The lower portion shows the saddle points as a function of constrained mass asymmetry $\alpha$ for $x=0.7$; the $\alpha$ values are in increments of 0.1, except for the largest value ($\alpha=0.93$).

At this point, we mention that it is impossible to extend these calculations much beyond $x=0.7$ for two reasons. For small values of $\alpha$, the saddle-point shape for $x\gtrsim 0.8$ has no well-defined neck, so it is impossible to unambiguously define $\alpha$. However, in the region of large $\alpha$, where one might expect a constrained saddle to exist (viz., Fig. 2), there is no solution to the constrained saddle-point problem for a maximum value of $x$ which depends on $\alpha$. Qualitatively, we can understand why no solution can exist for a large enough fissility. For the lighter systems, the configuration for large $\alpha$ is essentially the ground state of the larger fragment somewhat distorted in the polarizing field of the lighter fragment. For sufficiently heavy nuclei, the field of the light fragment distorts the heavy fragment so much that it is driven beyond its own fission barrier, and thus no saddle point can exist.

Finally, in Fig. 4 we show the shapes of the constrained macroscopic saddle points for the nucleus $^{208}$Bi for both the liquid-drop model and the Yukawa-plus-exponential model. In the liquid-drop model, this nucleus has fissility $x=0.6986$, so the results on the left-hand side of the figure are essentially the same as the shapes presented in Fig. 2 for $x=0.7$. We see that the behavior of the two models is similar to each other except for the familiar results that in the Yukawa-plus-exponential model the saddle points have larger necks, and their energies are lower than in the liquid-drop model.[61]

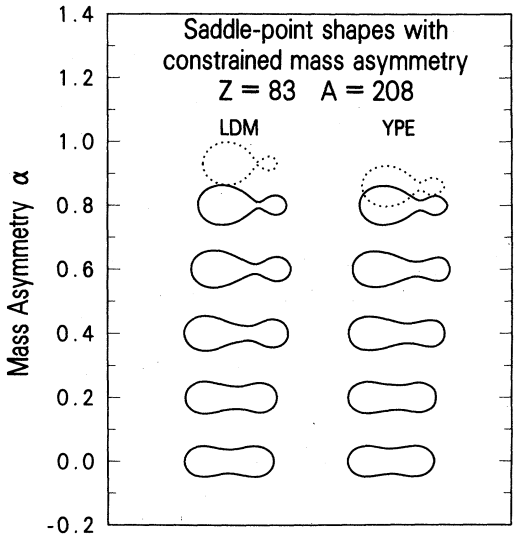


FIG. 4. Saddle-point configurations for the nucleus $Z=83$, $A=208$ as a function of constrained mass asymmetry $\alpha$ for two different models of the nuclear energy. The shapes on the left-hand side have the liquid-drop-model surface energy with fissility $x=0.7$, while those on the right-hand side have the Yukawa-plus-exponential double-folded nuclear energy and diffuse-surfaced charge distributions. The dotted shapes with very small neck radii occur at the largest values of $\alpha$ for which we are able to calculate.

## IV. SUMMARY

We have developed a general method for determining an extremum on a potential energy surface subject to an arbitrary number of constraints. The basic equations are formulated using Lagrange multipliers, and the extremum is obtained by iterating using a vector version of Newton's method. We then specialize the problem to a single constraint which can be, e.g., a multipole moment of the nuclear shape or a parameter specifying the mass asymmetry of the system. All of the calculations of this paper are done for the constraint of mass asymmetry which might typically represent the initial value of mass asymmetry of a particular heavy-ion reaction. Such calculations then give the conditional saddle points which are thought to enable one to distinguish theoretically fast fission processes from true compound nucleus formation.[20–23] The advantage of the present method is that the conditional saddle points can be calculated when the mass asymmetry function is an arbitrary function of the generalized coordinates. This should be contrasted with other studies[20–25] in which the mass asymmetry variable is one of the chosen generalized coordinates, in which case the conditional saddle points can be determined by simply fixing the asymmetry coordinate.

The results of this paper are obtained mainly with the liquid-drop-model surface energy. A study comparing the results using the liquid-drop model with those of the Yukawa-plus-exponential nuclear energy shows that for the latter one obtains a larger neck for a given mass asymmetry. However, the main conclusions of the paper do not depend on the type of macroscopic energy considered. In order to describe the nuclear shape which is assumed to be axially symmetric, we use two different parametrizations: (i) a model consisting of smoothly joined portions of three quadratic surfaces of revolution, and (ii) a Legendre polynomial expansion of the nuclear surface function.

We present our results showing the geometrical shapes and energies of the saddle-point configurations. In addition, we display the saddle points on $\sigma$-$r$ plots where $\sigma$ and $r$ represent, respectively, necking and separation degrees of freedom. We find that, for a given fissility $x$, as we increase the mass asymmetry $\alpha$ the moments of the system effectively behave like those of lighter nuclei. This occurs because, in a heavy-ion reaction appropriate to a given mass asymmetry, the effective entrance-channel Coulomb repulsion is proportional to $Z_1 \cdot Z_2$ where $Z_1$ and $Z_2$ are the projectile and target charges. Then, for a fixed total charge of the system, as $\alpha$ increases $Z_1 \cdot Z_2$ decreases giving rise to a less repulsive system. Also, the behavior of the energies of the conditional saddle points versus $\alpha$ depends upon whether the fissility is above or below the Businaro-Gallone point, $x_{BG}=0.396$. For $x<x_{BG}$ the energy always decreases monotonically with increasing $\alpha$. On the other hand, for $x>x_{BG}$, as $\alpha$ increases the energy first increases until it reaches a maximum corresponding to the Businaro-Gallone peaks after which it decreases. In the neighborhood of $x=x_{BG}$, the saddle-point energy with respect to $\alpha$ is very flat due to the coalescence at $\alpha=0$ of the Bohr-Wheeler mass symmetric saddle family with the Businaro-Gallone mass asymmetric saddle family. For $\alpha=0$ the conditional saddle point is always the Bohr-Wheeler saddle, while for $\alpha$ approaching 1 it corresponds to a single large sphere attached to an infinitesimally small sphere.

This research was supported by the U. S. Department of Energy under a contract with the University of California and Contract DE-AC05-840R21400 with Martin Marietta Energy Systems, Inc.

[1]W. J. Swiatecki, in *Proceedings of the International Conference on Nuclear Reactions Induced by Heavy Ions, Heidelberg, 1969,* edited by R. Bock and W. R. Hering (North-Holland, Amsterdam/American Elsevier, New York, 1970), p. 729.
[2]W. J. Swiatecki, J. Phys. Suppl. **33**, C5-45 (1972).
[3]W.J. Swiatecki and S. Bjørnholm, Phys. Rep. **4C**, 325 (1972).
[4]J. R. Nix, CERN Report No. CERN-70-30, 1970 (unpublished), Vol. 2, p. 605.
[5]J. R. Nix, Phys. Today **25**, No. 4, 30 (1972).
[6]J. R. Nix, Institute of Nuclear Research Report No. INR-P-1447/I/PL, 1972 (unpublished), Vol. 1, p. 299.
[7]J. R. Nix, Annu. Rev. Nucl. Sci. **22**, 65 (1972).
[8]A. J. Sierk and J. R. Nix, in *Proceedings of the Third International Atomic Energy Agency Symposium on the Physics and Chemistry of Fission, Rochester, New York, 1973* (IAEA, Vienna, 1974), Vol. II, p. 273.
[9]J. R. Nix and A. J. Sierk, Phys. Scr. **10A**, 94 (1974).
[10]J. R. Nix and A. J. Sierk, University of Milan report, 1975 (unpublished), p. 1.
[11]J. R. Nix and A. J. Sierk, Joint Institute for Nuclear Research Report No. JINR-D7-9734, 1976 (unpublished), p. 101.
[12]A. J. Sierk and J. R. Nix, Argonne National Laboratory Report No. ANL-PHY-76-2, 1976 (unpublished), Vol. I, p. 407.
[13]J. R. Nix and A. J. Sierk, Phys. Rev. C **15**, 2072 (1977).
[14]A. J. Sierk and J. R. Nix, Phys. Rev. C **16**, 1048 (1977).
[15]A. A. Amsden, A. S. Goldhaber, F. H. Harlow, P. Möller, J. R. Nix, and A. J. Sierk, IPCR Cyclotron Progress Report, Supplement 6, 1977 (unpublished), p. 235.
[16]A. J. Sierk, in *Proceedings of the International Symposium on Superheavy Elements, Lubbock, Texas, 1978,* edited by M. A. K. Lodhi (Pergamon, New York, 1978), p. 479.
[17]J. R. Nix, S. Afr. J. Phys. **1**, 103 (1978).
[18]J. R. Nix, in *Proceedings of the International Conference on Nuclear Interactions, Canberra, Australia, 1978,* edited by B. A. Robson (Springer, Berlin, 1978), p. 140.
[19]W. J. Swiatecki, Prog. Part. Nucl. Phys. **4**, 383 (1980).
[20]W. J. Swiatecki, Phys. Scr. **24**, 113 (1981).
[21]W. J. Swiatecki, CERN Report No. CERN-81-09, 1981 (unpublished), p. 781.
[22]W. J. Swiatecki, Nucl. Phys. **A376**, 275 (1982).
[23]S. Bjørnholm and W. J. Swiatecki, Nucl. Phys. **A391**, 471 (1982).
[24]J. Błocki and W. J. Swiatecki (unpublished).
[25]H. Feldmeier, in *Proceedings of the Xth International Workshop on Gross Properties of Nuclei and Nuclear Excitations, Hirschegg, Austria, 1982,* edited by H. Feldmeier (Technishche Hochschule, Darmstadt, 1982), p. 26.
[26]J. Błocki and M. Dworzecka, Bull. Am. Phys. Soc. **27**, 550 (1982).
[27]P. Bonche, K. T. R. Davies, B. Flanders, H. Flocard, B. Grammaticos, S. E. Koonin, S. J. Krieger, and M. S. Weiss, Phys. Rev. C **20**, 641 (1979).
[28]K. T. R. Davies, K. R. S. Devi, and M. R. Strayer, Phys. Rev. Lett. **44**, 23 (1980).
[29]K. T. R. Davies, K. R. S. Devi, and M. R. Strayer, Phys. Rev. C **24**, 2576 (1981).
[30]H. Stöcker, R. Y. Cusson, H. J. Lustig, A. Gobbi, J. Hahn, J. A. Maruhn, and W. Greiner, Z. Phys. A **306**, 235 (1982).
[31]H. Sann, R. Bock, Y. T. Chu, A. Gobbi, A. Olmi, U. Lynen, W. Müller, S. Bjørnholm, and H. Esbensen, Phys. Rev. Lett. **47**, 1248 (1981).
[32]R. Bock, Y. T. Chu, M. Dakowski, A. Gobbi, E. Grosse, A. Olmi, H. Sann, D. Schwalm, U. Lynen, W. Müller, S. Bjørnholm, H. Esbensen, W. Wölfli, and E. Morenzoni, Nucl. Phys. A **388**, 334 (1982).
[33]S. Bjørnholm, in *Proceedings of the Xth International Workshop on Gross Properties of Nuclei and Nuclear Excitations, Hirschegg, Austria, 1982,* edited by H. Feldmeier (Technische Hochschule, Darmstadt, 1982), p. 15.
[34]S. Bjørnholm, in *Proceedings of the Nuclear Physics Workshop, Trieste, Italy, 1981,* edited by C. H. Dasso, R. A. Broglia, and A. Winther (North-Holland, Amsterdam, 1982), p. 521.
[35]S. Bjørnholm, Nucl. Phys. **A387**, 51c (1982).
[36]S. Bjørnholm, Comments Nucl. Part. Phys. **11**, 9 (1982).
[37]J. R. Huizenga, J. R. Birkelund, W. U. Schröder, W. W. Wilcke, and H. J. Wollerscheim, in *Proceedings of the Third Adriatic Europhysics Study Conference on the Dynamics of Heavy-Ion Collisions, Hvar, Yugoslavia, 1981,* edited by N. Cindro, R. A. Ricci, and W. Greiner (North-Holland, Amsterdam, 1981), p. 15.
[38]H. Gäggeler, W. Brüchle, J. V. Kratz, M. Schädel, K. Sümmerer, G. Wirth, and T. Sikkeland, in *Proceedings of the Xth International Workshop on Gross Properties of Nuclei and Nuclear Excitations, Hirschegg, Austria, 1982,* edited by H. Feldmeier (Technische Hochschule, Darmstadt, 1982), p. 40.
[39]H. Gäggeler, T. Sikkeland, G. Wirth, W. Brüchle, W. Bögl, G. Franz, G. Herrmann, J. V. Kratz, M. Schädel, K. Sümmerer, and W. Weber, Z. Phys. A **316**, 291 (1984).
[40]W. Westmeier, R. A. Esterlund, A. Rox, and P. Patzelt, Phys. Lett. B **117**, 163 (1982).
[41]B. Sikora, J. Bisplinghoff, M. Blann, W. Scobel, M. Beckerman, F. Plasil, R. L. Ferguson, J. Birkelund, and W. Wilcke, Phys. Rev. C **25**, 686 (1982).
[42]K. Luetzenkirchen, University of Mainz, diploma work, 1982 (unpublished).
[43]D. H. E. Gross and L. Satpathy, Phys. Lett. B **110**, 31 (1982).
[44]K. H. Schmidt, P. Armbruster, F. P. Hessberger, G. Munzenberg, W. Reisdorf, C. C. Sahm, D. Vermeulen, H. G. Clerc, J. Keller, and H. Schulte, Z. Phys. A **301**, 21 (1981).
[45]C. Grégoire, C. Ngô, and B. Remaud, Phys. Lett. **B99**, 17 (1981).
[46]C. Grégoire, C. Ngô, and B. Remaud, Nucl. Phys. **A383**, 392 (1982).
[47]A. K. Dhar, Phys. Rev. Lett. **50**, 478 (1983).
[48]P. Fröbrich, Phys. Lett. B **122**, 338 (1983).
[49]K. T. R. Davies, A. J. Sierk, and J. R. Nix, Phys. Rev. C **28**, 679 (1983).
[50]K. T. R. Davies, A. J. Sierk, and J. R. Nix, in *Proceedings of the XIth International Workshop on Gross Properties of Nuclei and Nuclear Excitations, Hirschegg, Austria, 1983,* edited by H. Feldmeier (Technische Hochschule, Darmstadt, 1983), p. 135.
[51]K. T. R. Davies, A. J. Sierk, and J. R. Nix, in Proceedings of the International Winter Meeting on Nuclear Physics, Bormio, Italy, 1983, p. 255.
[52]K. T. R. Davies, A. J. Sierk, and J. R. Nix, in *Proceedings of the International Conference on Nuclear Physics with Heavy Ions, Stony Brook, New York, 1983,* edited by Peter Braun-Munzinger (Harwood Academic, New York, 1984), p. 57.
[53]J. R. Nix and A. J. Sierk, in Proceedings of the International Conference on Theoretical Approaches to Heavy-Ion Reaction Mechanisms, Paris, France, 1984.
[54]J. A. Maruhn, K. T. R. Davies, and M. R. Strayer, Phys. Rev. C. (to be published).
[55]S. Trentalange, S. E. Koonin, and A. J. Sierk, Phys. Rev. C. **22**, 1159 (1980).
[56]H. Goldstein, *Classical Mechanics* (Addison-Wesley, Reading,

Mass., 1959), p. 318.
[57]K. T. R. Davies, A. J. Sierk, and J. R. Nix, Phys. Rev. C **13**, 2385 (1976).
[58]K. T. R. Davies and A. J. Sierk, J. Comput. Phys. **18**, 311 (1975).
[59]W. D. Myers and W. J. Swiatecki, Ark. Fys. **36**, 343 (1967).
[60]H. J. Krappe, J. R. Nix, and A. J. Sierk, Phys. Rev. Lett. **42**, 215 (1979).
[61]H. J. Krappe, J. R. Nix, and A. J. Sierk, Phys. Rev. C **20**, 992 (1979).
[62]J. R. Nix, Nucl. Phys. **A130**, 241 (1969).
[63]U. L. Businaro and S. Gallone, Nuovo Cimento **1**, 629 (1955); **1**, 1277 (1955).